Small Angle Neutron Scattering Studies of the Counterion Effects on the Molecular Conformation and Structure of Charged G4 PAMAM Dendrimers in Aqueous Solutions

Wei-Ren Chen,[†,‡,||] Lionel Porcar,[§,||] Yun Liu,[§,||] Paul D. Butler,[||] and Linda J. Magid*[,‡]

Spallation Neutron Source, Oak Ridge National Laboratory, Oak Ridge, Tennessee 37831, Department of Chemistry, the University of Tennessee, Knoxville, Tennessee 37996-1600, The NIST Center for Neutron Research, National Institute of Standards and Technology, Gaithersburg, Maryland 20899-8562, and Department of Materials Science and Engineering, University of Maryland, College Park, Maryland 20742-2115

Received November 17, 2006; Revised Manuscript Received May 4, 2007

ABSTRACT: The structural properties of generation 4 (G4) poly(amidoamine) starburst dendrimers (PAMAM) with an ethylenediamine (EDA) central core in D_2O solutions have been studied by small-angle neutron scattering (SANS). Upon the addition of DCl, SANS patterns show pronounced inter-particle correlation peaks due to the strong repulsion introduced by the protonation of the amino groups of the dendrimers. By solving the Ornstein−Zernike integral equation (OZ) with hypernetted chain closure (HNC), the dendrimer−dendrimer structure factor $S(Q)$ is determined and used to fit the experimental data, where Q is the magnitude of the scattering wave vector. Quantitative information such as the effective charge per dendrimer and the radius of gyration, R_G, at different pD values is obtained. The results show that R_G only changes by about 4% when the pD value varies from 10.25 to 4.97, and significant counterion association/condensation occurs, strongly mediating the inter-dendrimer interaction. The influence of interplay between counterions and molecular protonation of dendrimers imposes a strong effect on the dendrimer conformation and effective interaction. Although the change of R_G is very small, careful analyses of the high Q data and fitting parameters indicate a possible internal structure change of a dendrimer when the amino groups are progressively charged.

I. Introduction

Dendrimers are regularly branched spherical macromolecules with well-defined hierarchical architectures built from multifunctional core molecules. They can be synthesized iteratively. In each sequence a new concentric shell consisting of terminal groups is added and leads to the next generation of dendrimers. With each ensuing generation, the size and the molecular weight increases approximately linearly but the number of the growing terminal groups increases exponentially. Several intrinsic properties, including small and well-defined molecular architectures on the nanometer length scale; high structural and physicochemical uniformity; and the ability to be functionalized to fit specific uses through the modification of the peripheral multivalent surface, interior region and core molecule, makes dendrimers promising candidates for an expanding range of applications.[1−4]

Among over 100 different dendrimer compositions, the family of the polyamidoamine dendrimers (PAMAM) with ethylenediamine (EDA) cores and amino group is the first one to be commercially available.[5,6] There has been an increasing interest in their potential medical applications due to the combination of aforementioned unique properties with high biocompatibility, low immunogenicity, and ease of syntheses on a large scale with reasonable manufacturing costs.

One of the proposed uses is that, by encapsulating exogenous materials, such as the therapeutic drug molecules, within the internal cavities, the dendrimer molecule may provide a practical means to facilitate the delivery of dendrimer−drug complexes to certain target areas.[7,8] In this application, the dendrimer molecular conformation is expected to play a key role in determining to what extent the accommodation of the foreign molecules can build up. With the peripheral primary and interior tertiary amino groups the protonation of PAMAM dendrimer molecules can be precisely modulated by adjusting the pH value of the solution. This tunable repulsion due to the charged amino groups promises the possibility of controlling the molecular conformation by varying the physiological conditions of solutions.

Computationally this scenario was first exploited by Welch and Muthukumar.[9] In their work, the bead-and-spring model, where a unit charge is associated with each bead representing the amino groups, was developed and based on this model, Monte Carlo (MC) simulations were performed to mimic the highly charged PAMAM dendrimers in aqueous solutions. A nontrivial structural dependence of the charged dendrimers on the ionic strength of the solutions was predicted: Upon decreasing the salt concentration, they showed that the dendrimer radial density profile undergoes a conformational transition from a compact profile to an extended one. In a certain range of ionic strength and pH, the radius of gyration R_G was predicted to vary up to a factor of 1.8. In the above research the solvent was treated as a continuous medium and the effect of counterions was not considered explicitly. Therefore, it is conjectured that the dependence of the intramolecular conformation of charged dendrimers on the ionic strength or pH of the solution may be much more complicated than the scenario depicted by this highly simplified coarse-grained approach. More recently, there have been several molecular dynamics (MD) attempts,

* Corresponding author. E-mail: lmagid@utk.edu.
† Spallation Neutron Source, Oak Ridge National Laboratory.
‡ Department of Chemistry, the University of Tennessee.
|| The NIST Center for Neutron Research, National Institute of Standards and Technology.
§ Department of Materials Science and Engineering, University of Maryland.

10.1021/ma0626564 CCC: $37.00
Published on Web 07/06/2007

each with a variable degree of success, to improve the computational results.[10−17] Despite the apparent numerical discordances due to the different simulation algorithms employed, they all seem to lead to a qualitatively consistent conclusion.[10−13,15−17] Protonation of the amino groups introduces an effect similar to that demonstrated by Welch and Muthukumar's mean-field approach, namely a conformational change. Not found in the mean-field simulation results, but revealed by recent atomic resolution molecular dynamics simulations is that by considering the water molecules and counterions explicitly, the swelling of the dendrimer molecule cannot be attributed merely to the pH effect. Instead, it manifests the collective effect of the presence of the water molecules within the interior cavities and the counterions attracted onto the molecule as well.[12,18] However, due to the constraints of current computer power, the best simulated scenario is still essentially different from the real physicochemical condition.[19] Moreover, experimental evidence suggests an invariance of the molecular conformation of generation 8 (G8) dendrimers in D_2O upon increasing the protonation, a contradictory picture to the computational predictions.[20] Therefore, the harder question of whether under the experimental conditions the dependence of the dendrimer conformation on the counterion effect and ionic strength is consistent with the computational predictions has not been answered unambiguously.

It is therefore interesting and important to study and characterize the structure and the effective interaction of these charged dendrimers in aqueous solutions for the cases in which computer simulation results are available for comparison. Because of the limit of computation power, most computational works simulate the molecular conformation changes of dendrimers of generation 1 to generation 5.[10−15] In this paper, we provide the first report of quantitative information concerning conformational changes of generation 4 (G4) PAMAM dendrimers in D_2O for the pD value ranging from 10.25 to 4.97.

Together with the conformation change, the counterions associated with each dendrimer are also obtained in the current study through the relations between the structure factor $S(Q)$ and the inter-particle interaction characterized by the effective pair potential model $V_{eff}(r)$, which takes into account solvent effects in an implicit manner. In general the link between the structure factor $S(Q)$ (or equivalently pair correlation function$g(r)$) and the effective interaction is provided by solving the Ornstein−Zernike integral equation (OZ)[21] with a specific closure. The $S(Q)$ obtained by solving the OZ equation has been proved to be accurate for various potentials and a suitable choice of closures. It can be immediately appreciated that the effective inter-particle interaction stemming from this one-component picture depends sensitively on the thermodynamic state of the whole system. For an electrolyte solution such as the charged dendrimer solution, the most relevant physical quantities in determining the thermodynamic equilibrium state is the excluded volume of the particle, the charges carried by the particle and the ionic strength of the medium. In comparison to the globular colloidal systems such as protein solutions, it is essential to take into account its unique dual structural characteristics by using SANS technique to study the structure of charged dendrimers solutions: In addition to the overall globular shape like the traditional colloids, dendrimer molecules possess a polymer-like feature at the molecular length scale. In particular, the local structural openness, combined with the association of counterions with the dendrimer molecule due to the electrostatic attraction when the amino groups are protonated, not only extensively redistributes the counterions in the solutions and therefore inevitably alters the effective charge carried by a dendrimer molecule and the ionic strength of the solution, but it may also contribute to the aforementioned predicted conformation transition and result in the variation of the dendrimer molecular size and the total dendrimer volume fraction. The charged dendrimer solutions have been the subject of several small angle scattering studies.[20,22−25] However, a quantitative description of the counterion effect does not exist. One of the questions motivating the present study is to understand the roles of the counterions, the effective charges carried by the dendrimer molecule and its intrinsic molecular conformation controlling the inter-dendrimer interaction and consequently the final equilibrium structure.

The present work advances the current state of understanding in the following ways: we use the inter-dendrimer structure factor $S(Q)$, obtained by solving the OZ equation numerically with the hypernetted chain approximation (HNC)[21] and the intra-dendrimer structure factor $P(Q)$ to analyze the SANS intensity distributions for various thermodynamic states of the charged dendrimer solutions. We demonstrate how the effect of the counterions on the dendrimer conformation and effective interaction can be understood when the fluctuation of ionic strength due to the interplay of the electrostatic attraction between the counterions and the protonated dendrimer molecules are specifically included into the model of charged dendrimer solutions.

This paper is organized as follows. In section II, we describe the preparation of the charged dendrimer solutions and the SANS experiments. The modeling of the SANS absolute intensity, including the introduction of $P(Q)$, $S(Q)$, OZ-HNC approach, and the generalized one-component macroion theory (GOCM) used to incorporate the ionic strength into the model, are introduced in section III. Section IV presents the model fitting results in detail. We end with a few concluding remarks in section V.

II. Materials and Methods

Materials. Newly available higher purity biomedical grade Generation 4 (G4) polyamidoamine starburst dendrimers (PAMAM) with ethylenediamine (EDA) cores were purchased from Dendritech Inc., Midland, MI.[26] Deuterium chloride (catalog number DLM-54-25) and deuterium oxide (catalog number DLM-6-10X1) were obtained from Cambridge Isotope Laboratories, Inc., Andover, MA.[26] The solutions were filtered (Whatman Anotop 25 0.02 μm, category number 6809-4102, batch no. 05003L)[26] and checked by dynamic light scattering prior to SANS measurements to make sure to completely remove any amount of possible aggregates. The dendrimer concentration of the samples used in the SANS experiment was kept at a constant value of 0.0225 g/mL. *In the current report, the added deuterium chloride used to protonate the amino groups is represented by* α*, the molar ratio of acid to the primary amino groups.*[27] The relation between α and the pD values of G4 charged dendrimer solutions studied in this report is given in Figure 1a. The chloride concentration as a function of pD value is given in Figure 1b as well.

It is important to realize that the pH of a solution in H_2O is different from its corresponding pD in a D_2O solution when $[H^+] = [D^+]$. It is generally agreed that pD = pH + 0.41,[28] where pH is the value measured with a conventional pH meter (a METTLER TOLEDO S20 SevenEasy pH meter is used in this current study[26]). This should be kept in mind when discussing the relation between the pD and the charge.

Small-Angle Neutron Scattering (SANS). SANS measurements were performed on the NG-3 SANS instruments at the NIST Center for Neutron Research. The wavelength of the incident neutrons was 6.0 Å, with wavelength spreads, $(\Delta\lambda)/(\lambda)$, of 15%. The scattering wave vector Q ranges from 0.0045 to 0.45 Å^{-1}. The samples were

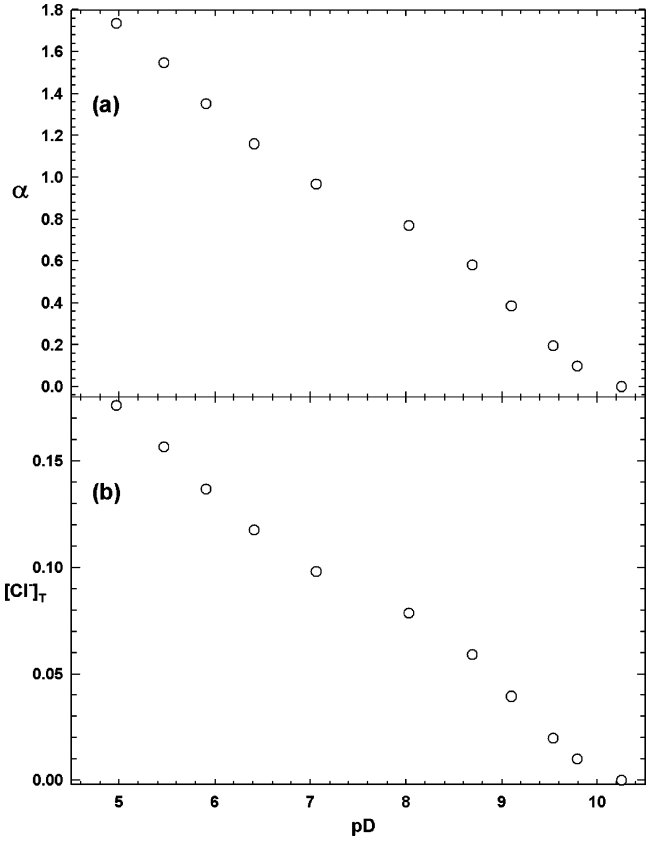

Figure 1. (a) pD value of PAMAM dendrimers of generation 4 in D_2O solutions with concentration of 0.0225 g/mL as a function of α using DCl. (b) Total molar concentration of chloride added in the solutions as a function of pD is given in the bottom panel.

contained in a 2 mm path length quartz cells obtained from Hellma Optik GmbH Jena, Jena, Germany (category number 120 mat. code QS),[26] and all the experiments were performed at a controlled temperature of 23.0 ± 0.1 °C. The measured intensity was also corrected for detector background and sensitivity and for scattering contributed from the empty cells and placed in an absolute scale using a direct beam measurement.[29]

III. Theoretical Basis

SANS scattering intensity $I(Q)$ obtained from colloidal suspensions can be expressed as[30]

$$I(Q) = n_D {\nu_D}^2 (\bar{\rho} - \rho_s)^2 P(Q) S(Q) \quad (1)$$

where n_D gives the number density of the dendrimers in the solutions, ν_D the volume of a single dendrimer molecule, $\bar{\rho} - \rho_s$, the difference of the scattering length density between the dissolved dendrimers and the solvent, $P(Q)$ the normalized dendrimer form factor, and $S(Q)$ the structure factor. Equation 1 is usually called the factorization approximation.

Model of the Intra-Particle Structure Factor *P*(*Q*). There has been much interest in understanding the molecular density profile of dendrimers since their first synthesis: From an intuitive point of view, dendrimers can be viewed as macromolecules with empty interior region and peripheral region with highest segmental density. This so-called "dense-shell" picture is supported by the theoretical work of de Gennes et al.[31] On the other hand, in previous scattering experiments a uniform density picture was first used to model the molecular density profile of dendrimer molecules and their charged state in aqueous solutions.[20] In several recent comprehensive reviews,[32−34] after summarizing a range of consistent experimental, computational and theoretical evidence, Ballauff and Likos conclude that the dense-core model proposed by Lescanec and Muthukumar[35] is indeed an unequivocal characterization of the dendrimer molecular density profile. Consistent with this picture, Rathgeber and co-workers[36] propose a semiempirical model for the normalized dendrimer form factor $P(Q)$, which is similar to the form factor model for star polymers previously given by Pedersen:[37]

$$P(Q) \equiv \left\{ \frac{3}{(QR)^3} [\sin(QR) - QR\cos(QR)] \exp\left(-\frac{Q^2\sigma^2}{4}\right) \right\}^2 + a_b P_{fluc}(Q, R_G) \quad (2)$$

Schematically, its physical meaning can be best depicted with the following argument: Unlike the well-defined interface characterized by the Q^{-4} Porod decay, the scattering length density is found to change continuously across the dendrimer-solvent interface due to the unique cascade structure of the dendrimer molecules. To model the scattering contribution from an object with this so-called diffuse interface,[38−40] the local variation of the scattering length density profile is treated as a step profile representing a solid sphere with radius R, as used in ref 20, convoluted with a smooth function (a Gaussian distribution with standard deviation σ is chosen in their model), as shown in the first term of the right-hand side of eq 2. The second term is introduced to incorporate the scattering contribution from the intra-dendrimer density fluctuations dominating at large Q, with a_b giving the ratio of its contribution to $P(Q)$ normalized to the first term. It is important to note that, for all the SANS intensity distributions reported here, except for the $\alpha = 0$, the presence of the structure factor $S(Q)$ due to the screened Coulombic inter-dendrimer interaction considerably complicates the inverse Fourier transform (IFT) approach, adopted by Rathgeber and co-workers[36] for the case of dilute uncharged dendrimer solutions, to obtain the radius of gyration R_G precisely. Therefore, in this study we propose an alternative solution to bypass this highly nonlinear mathematical approach. First, we define the first term on the right-hand side of eq 2 as

$$A(Q,R,\sigma)^2 \equiv \left\{ \frac{3}{(QR)^3} [\sin(QR) - QR\cos(QR)] \exp\left(-\frac{Q^2\sigma^2}{4}\right) \right\}^2 \quad (3)$$

The radius of gyration R_G is defined as

$${R_G}^2 \equiv \frac{\int \Delta\vec{r}^2 \rho(\vec{r}) d^3}{\int \rho(\vec{r}) d^3} \quad (4)$$

where $\rho(\vec{r})$ is the intra-particle scattering length distribution function. Then R_G can be calculated and expressed as a simple analytical function of R and σ:

$${R_G}^2 \equiv {R_G}^2(R,\sigma) = \frac{\nabla_{\vec{Q}}^2 A(Q,R,\sigma)|_{Q\to 0}}{A(Q=0,R,\sigma)} = \frac{3}{10}(2R^2 + 5\sigma^2) \quad (5)$$

During the derivation, the contribution from the second term of eq 2 is ignored due to its negligible small value when Q approaches zero.

The intramolecular scattering length density profile in this proposed model can be schematically characterized by a smooth

decay from the central plateau region along the radial direction to its periphery with a Gaussian dependence on length.

Model of the Inter-Particle Structure Factor *S*(*Q*). The OZ integral equation gives the exact mathematical relation in terms of different spatial distribution functions:[21]

$$h(r) = c(r) + n_D \int c(|\vec{r}' - \vec{r}\,|)h(\vec{r}')d^3\,\vec{r}', \quad \text{where } r \equiv |\vec{r}| \tag{6}$$

In eq 6, $h(r) \equiv g(r) - 1$, where $g(r)$ is the pair correlation function, gives the total correlation function between two given particles and is the sum of two contributions: $c(r)$ which measures the "direct" correlation between the two particles, plus the "indirect" effect, the additional contribution to $h(r)$ from correlations transmitted between these two particles via a third particle, which is expressed through the integral of the direct correlation function $c(r)$ with the total correlation function $h(r)$ over all the possible configurations of the third particle and multiplied by the number density of particles n_D.

The inter-particle structure factor, $S(Q)$, which is defined as

$$S(Q) \equiv 1 + n_D \int h(r) \exp(-i\vec{Q}\bullet\vec{r})d^3\,\vec{r} \tag{7}$$

can be obtained by solving eq 6 with a suitable closure relation which relates the direct correlation function $c(r)$ back to the total correlation function $h(r)$ and is highly dependent on the nature of the effective pair potential $V(r)$. In the current report, the structure factor $S(Q)$ is obtained by solving eq 6 numerically with the hypernetted chain (HNC) approximation:[21]

$$c(r) = -\frac{V(r)}{k_B T} + h(r) - \ln[1 + h(r)], \quad r > d \tag{8}$$

$$h(r) = -1, \quad r < d \tag{9}$$

where $V(r)$ is the effective pair potential between any two given particles and d is the particle diameter due to the excluded volume effect. During the model fitting, the effective hard-core radius is defined as R_G so that $d = 2R_G$. We have tried to let the hard-core diameter vary as a fitting parameter, however, the results for small and large α show that the ratio between the fitted hard-core radius and R_G is about one. We then assign the hard-core radius as R_G in all the fittings, which show excellent fitting results.[41] The effective volume of a single dendrimer molecule is then defined as $\nu_D \equiv (4\pi/3)R_G^3$. Theoretically speaking, dendrimer molecules have been considered as soft colloids with soft-core interacting potential. An experimental investigation of the soft-core properties of dendrimers is ongoing, which will be addressed in our future paper. The current research focuses on studying the low concentration charged dendrimer solutions, and it is expected that under this condition the current treatment of dendrimer molecules with hard-core potential should be a fairly reasonable approximation.

The OZ-HNC approach has been previously applied to study the spatial counterion-macroion and macroion−macroion correlations in aqueous solutions of ionized colloids including charged micellar systems and globular protein molecules in aqueous solutions.[42−44] These previous works suggest that in terms of accuracy and efficiency it is well suited to provide information about effective inter-macroion interaction for highly charged systems, such as aqueous solutions of charged dendrimer molecules, interacting via the repulsive screened Coulombic potential $V_{SC}(x)$ which is specified by the Yukawa form:

$$V_{SC}(x) = -K_1 \frac{\exp[-Z_1(x-1)]}{x}, \quad \text{when } x > 1 \tag{10}$$

where K_1 is the interaction strength, normalized by thermal energy k_BT, the interaction distance is x and normalized to the particle diameter. The normalized interaction range is given as Z_1^{-1}.

In this study, we calculate the screened Coulombic repulsive interaction potential directly using a given effective charge number of a dendrimer molecule and the ionic strength of the medium. The effective charge number of a single dendrimer is derived from K_1 and Z_1 via the generalized one-component macroion theory (GOCM).[45−46] The application of GOCM theory, a equivalent approach which is named as rescaling mean spherical approximation (RMSA) in ref 45, to compute the effective charge number for a protein in solutions with volume fraction up to 0.2 has been demonstrated to be successful.[46]

The Derjaguin−Landau−Verwey−Overbeek (DLVO) theory has been widely used to describe the effective pair interaction of monodispersed charged colloidal systems.[47] However, the GOCM approach is chosen in the current research and the reasons are twofold: first, it is found in the dilute limit of colloidal concentration that both DLVO and GOCM give quantitatively an identical measure of effective charge numbers. Second, the DLVO theory overestimates the average charge number when applied to a charged colloidal system with higher volume fraction.[45−46] While we currently are presenting the data obtained from the samples with low dendrimer concentration (0.0225 g/mL), work is in progress to analyze the data obtained from charged dendrimer solutions with much higher concentration (in a concentration range of 0.0225 to 0.2 g/mL). To avoid any possible inconsistencies of data interpretation with future publications, we deliberately choose to adopt the GOCM theory.

Here we briefly present the modified equations necessary to relate the potential parameters K_1 and Z_1 to the number of a single dendrimer's effective charge, including the effect of counterion association. According to the results of GOCM, the repulsive screened Coulombic potential between two charged dendrimers is given as

$$V_{GOCM}(x) = \frac{Z_{ED}{}^2 e^2}{\epsilon(2R_G)} Y^2 \frac{\exp(-kx)}{x} \tag{11}$$

where ϵ is the dielectric constant of the medium, e the electronic charge, and Z_{ED} the effective charge number of a dendrimer molecule defined as

$$Z_{ED} \equiv Z - z_{CD} \tag{12}$$

where z_{CD} is the average number of counterions associated with a dendrimer molecule and Z the average number of protonated amino groups of a dendrimer molecule. For a given DCl acid concentration, it is determined by the overall charge neutrality and is represented by the following formula

$$Z = \frac{N_A}{n_D}([Cl^-] + [OH^-] - [D^+]) \tag{13}$$

where N_A is Avogadro's number. The parameter Y appearing in eq 11 is expressed as

$$Y \equiv \cosh\left(\frac{k}{2}\right) + U\left[\left(\frac{k}{2}\right)\cosh\left(\frac{k}{2}\right) - \sinh\left(\frac{k}{2}\right)\right] \tag{14}$$

where

$$U = \mu\left(\frac{k}{2}\right)^{-3} - \gamma\left(\frac{k}{2}\right)^{-1} \tag{15}$$

$$\mu = \frac{3\phi_D}{1-\phi_D} \tag{16}$$

$$\phi_D = n_D v_D = \frac{4n_D\pi}{3} {R_G}^3 \tag{17}$$

$$\gamma = \frac{2\mu + G}{2 + 2\mu + G} \tag{18}$$

and G is obtained by solving the following equation

$$G^2 = k^2 + \frac{4{t_0}^2}{(2 + 2\mu + G)^2} \tag{19}$$

given

$${t_0}^2 = \frac{24{Z_{ED}}^2 e^2 \phi_D}{k_B T \epsilon R_G} \tag{20}$$

$$k^2 = \left(\frac{8\pi e^2 I_S N_A}{10^3 k_B T}\right) {R_G}^2 \tag{21}$$

where I_S is the ionic strength of the medium defined as

$$I_S = \frac{1}{2}\left[[D^+] + [OH^-] + \frac{1}{(1-\phi_D)}\left([Cl^-] - \frac{n_D}{N_A} z_{CD}\right)\right] \tag{22}$$

Therefore, the Yukawa potential parameters K_1 and Z_1 defined in eq 10 can be expressed in terms of the GOCM parameters as

$$K_1 = -\frac{{Z_{ED}}^2 e^2}{\epsilon(2R_G)} Y^2 \exp(-k) \tag{23}$$

and

$$Z_1 = -k \tag{24}$$

Furthermore, we are aware of the fact that like all other ion selective electrodes, the pH meter does not measure the deuteron concentration, but its activity, the effective deuteron concentration. Namely it gives

$$a_D = \gamma_D [D^+] \tag{25}$$

where a_D represents the deuteron activity and is a function of total ionic strength of the electrolyte solution, and γ_D is the deuteron activity coefficient in solutions. Attempts have been made to take into account the effect of the total ionic strength of the solution such as incorporating the ionic interaction equations[48] into the algorithm to calculate the correct deuteron concentration iteratively during the fitting procedure. The importance of this consideration can be immediately appreciated from eq 22 by noticing the mathematical relationship among the deuteron concentration, the ionic strength of medium, the number of associated counterion,s and, consequently, the effective charge number of a single dendrimer molecule. However, in the range of pD values studied in this current paper the ratio of the free deuteron concentration to the chloride concentration is generally less than 10^{-4}. Consequently, it is found that the influence of the difference between the measured deuteron activity and the real deuteron concentration in solution on the final fitting results is insignificant, especially for the cases where $\alpha < 0.97$.

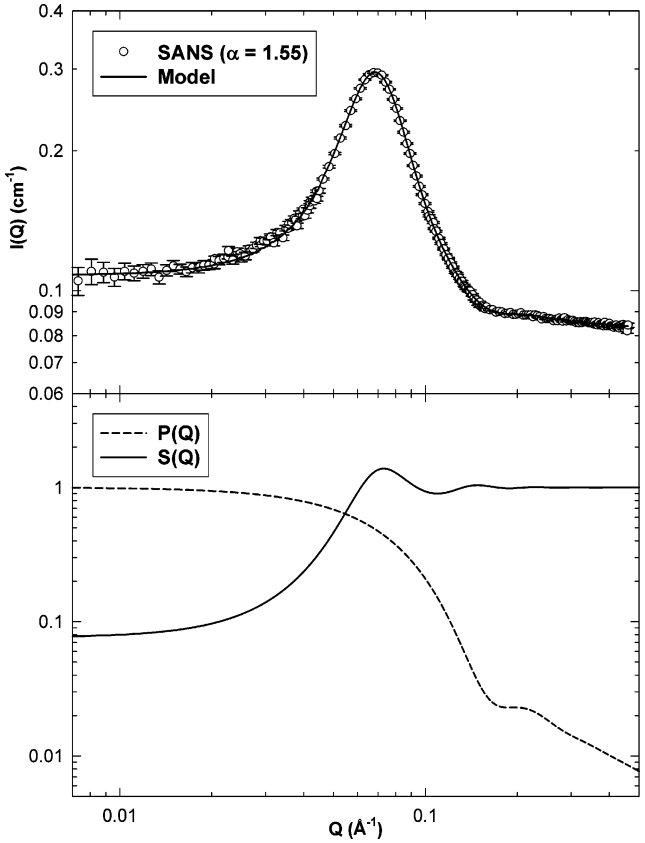

Figure 2. Upper panel: SANS intensity distribution obtained from PAMAM dendrimers of generation 4 in D_2O solutions with concentration of 0.0225 g/mL at $\alpha = 1.55$ on an absolute scale and its fit taking into account the incoherent background and the effect of the resolution function. Lower panel: corresponding normalized intra-particle structure factor $P(Q)$ and the inter-particle structure factor $S(Q)$.

Similar to ref 49, $(\bar{\rho} - \rho_s)^2$ in eq 1 is determined by fitting the SANS result obtained from a dilute neutral solution (0.005 g/mL in D_2O). It is also found that, in the current research for the charged G4 PAMAM dendrimer solutions at 0.0225 g/mL with different α values, when $(\bar{\rho} - \rho_s)^2$ is treated as a fitting parameter, only a slight variation of the value obtained at 0.005 g/mL is observed.

In addition to the predetermined experimental parameters including the dendrimer number density n_D and the concentrations of different ions, which can be calculated precisely from the amount of dendrimers, deuterium chloride and deuterium oxide present in the solutions, introducing the concept of the effective hard-core diameter and expressing R_G analytically in terms of R and σ enables us to obtain unambiguous and physically reasonable and consistent results by using five fitting parameters: *the incoherent background, the average number of counterions associated with a single dendrimer molecule z_{CD}, the weighting parameter a_b, R and σ for the normalized form factor P(Q)* in our fitting formula given by eq 1. During all the fitting, the instrument resolution has also been taken into consideration.

IV. Results and Discussion

Figure 2 displays an example of the SANS model fitting: A double logarithmic representation of the SANS absolute intensity of 0.0225 g/mL G4 PAMAM dendrimers solutions with $\alpha = 1.55$ is given in the top panel where symbols represent the

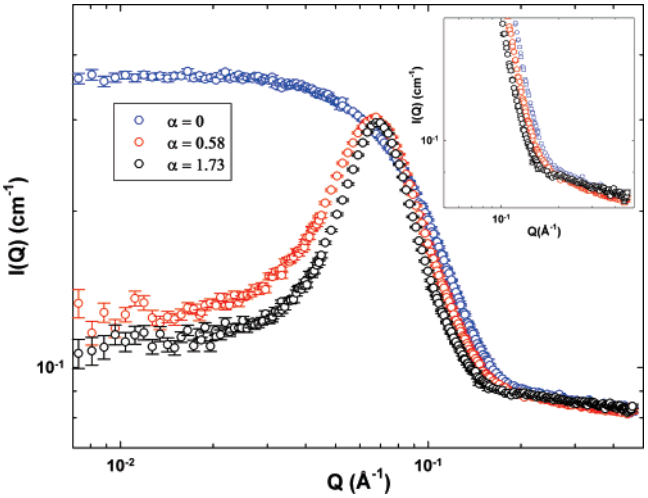

Figure 3. Comparison of the SANS scattering intensities of PAMAM dendrimers of generation 4 in D_2O solutions with concentration of 0.0225 g/mL obtained at $\alpha = 0$, 0.58, and 1.73 respectively. The enlarged high-Q parts of the scattering intensities are given in the inset.

experimental spectrum and the curve the model fitting result. The corresponding normalized intra-particle structure factor $P(Q)$ and inter-particle structure factor $S(Q)$ are given in the bottom panel. As pointed out in section III, $P(Q)$ is calculated from a semiempirical equation based on the dense-core fuzzy-ball model and $S(Q)$ is calculated by the OZ-HNC approach. The observed SANS intensity distributions are the product of these two functions. It is clear that the interaction peak in the SANS data is primarily due to the first-order diffraction peak of $S(Q)$. Another important point is the fact that $S(Q)$ becomes relatively smooth when $Q > 0.1$ Å^{-1}, implying that in this region $I(Q)$ is dominated by the contribution of $P(Q)$.

Figure 3 shows the SANS intensity distributions of G4 PAMAM dendrimers dispersed in D_2O with concentration fixed at 0.0225 g/mL and at various α values (The corresponding pH values for $\alpha = 0$, 0.58, and 1.73 are 10.25, 8.69, and 4.97 respectively). Two qualitative features are noticed: First, upon increasing the level of dendrimer protonation by adding DCl, the correlation peak becomes more pronounced. Second, contrary to the substantial variation of the SANS absolute intensity occurring in the low-Q region due to the increasing protonation of dendrimer molecules, the high-Q scattering intensity distributions for different α values are seen to be rather similar. As pointed out in the example given in Figure 2, in this high- Q region $I(Q)$ is dominated by the $P(Q)$ contributions. This invariance implies that the fluctuation of molecular conformations of G4 PAMAM dendrimers in aqueous solutions due to the variation of pH values (ranging from 4.97 to 10.25 in the current study) is not obvious. This preliminary observation seems to be consistent with the insensitivity of the molecular conformation of G8 PAMAM dendrimers in D_2O to the variation of the pH value found by Nisato and co-workers.[20] However, the quantitative change of the conformation can only be obtained by fitting the experimental SANS results.

A series of SANS intensity distributions (blue symbols) obtained from G4 PAMAM dendrimer solutions with different level of molecular protonation, their theoretical fits and corresponding scaling plots,[50−52] are given in Figures 4 and 5. The dendrimer concentration of the solutions is kept constant at 0.0225 g/mL after adding the acid. These figures clearly show that the combination of the modified dense core/fuzzy ball form factor $P(Q)$, the inter-particle structure factor $S(Q)$ obtained from the OZ-HNC approach and the incorporation of the effect of counterion association indeed renders satisfactory and consistent agreements with the corresponding SANS experimental results. It is important to qualitatively rationalize the current success: Similar to other charge-stabilized colloidal suspensions, the overall structure of the charged dendrimers in aqueous solutions is essentially determined by the collective interaction among the suspending charged dendrimers, the D_2O molecules and various co-ions and counterions. Hence the complexity of a complete statistical mechanical description is apparent. In general a coarse-grained approach, in which the information regarding degree of freedom of microions is contracted and the structural description of such a system is based on the spatial arrangement of the charged colloids defined by an effective pairwise potential, is popularly adopted to analyze the experimental observations, such as the methodology presented in the current report. However, the subject is often complicated by several factors, such as the variation of effective charge carried by a colloidal particle, even if the particle size is monodispersed,[53] uneven colloidal charge distribution,[54] and many-body effects.[55] The success of the current effective one-component model in describing the experimental observations validates the application of this highly simplified approach in the low dendrimer concentration limit where the aforementioned factors are expected to be negligibly small.[56]

Intramolecular Structure. The information about the molecular conformation is first presented: In Figure 6, the conformational information on G4 PAMAM dendrimers in D_2O solutions as a function of the molecular protonation is displayed. The variation of the intra-particle structure factor $P(Q)$ parameters R and σ as well as the radius of gyration R_G as a function of α is shown in the upper panel. The SANS model fitting suggests that, when α increases from 0 to 1.73 (pD value drops from 10.25 to 4.97), only a slight increase of R_G (less than 4%, indicated by the empirical fitting curve $R_G = 20.88 + 0.42\alpha$ Å) is observed. In other words, R_G is found to be insensitive to the variation of pD value of solutions within the α range studied. Quantitatively, this discovery is less significant in comparison with various computational predictions aforementioned, but consistent with the SANS experimental results obtained from the G8 dendrimers in aqueous solutions[20] and the conclusion of theoretical calculations, based on a mean-field model approximating the electrostatic interactions by Poisson−Boltzmann (PB) equation, for the G4 dendrimers within a certain pH range.[57]

Despite the essential invariance of R_G, the change of the molecular conformation is perceptible: A gradual increase of R (red symbols) and a simultaneous decrease of σ (black symbols) are observed. This implies that the dendrimer molecule undergoes a significant internal structural change during the protonation process. The ratio of σ/R as a function of α is given in the bottom panel. When $\alpha = 0$, the value of σ/R is found to be 0.53, which agrees with the value for the neutral G4 PAMAM dendrimer molecules in methanol.[36] Experimentally, it has been shown the ratio of σ/R decreases upon increasing the dendrimer generation and a stepwise transition for σ/R occurs when the generation number increases from 5 to 6.[36] In our experiment it is found that when $\alpha = 1.73$, the ratio σ/R is reduced to 0.27, which is about the value for a neutral G6 dendrimer in methanol. It is seen that the effect of molecular protonation in D_2O produces a similar effect as the increased generation number for neutral dendrimer in good solvent. Signaled by the evolution of σ/R as a function of α, it is also important to note that despite the invariance of the effective inter-dendrimer interaction potential within the α range where the tertiary amino groups

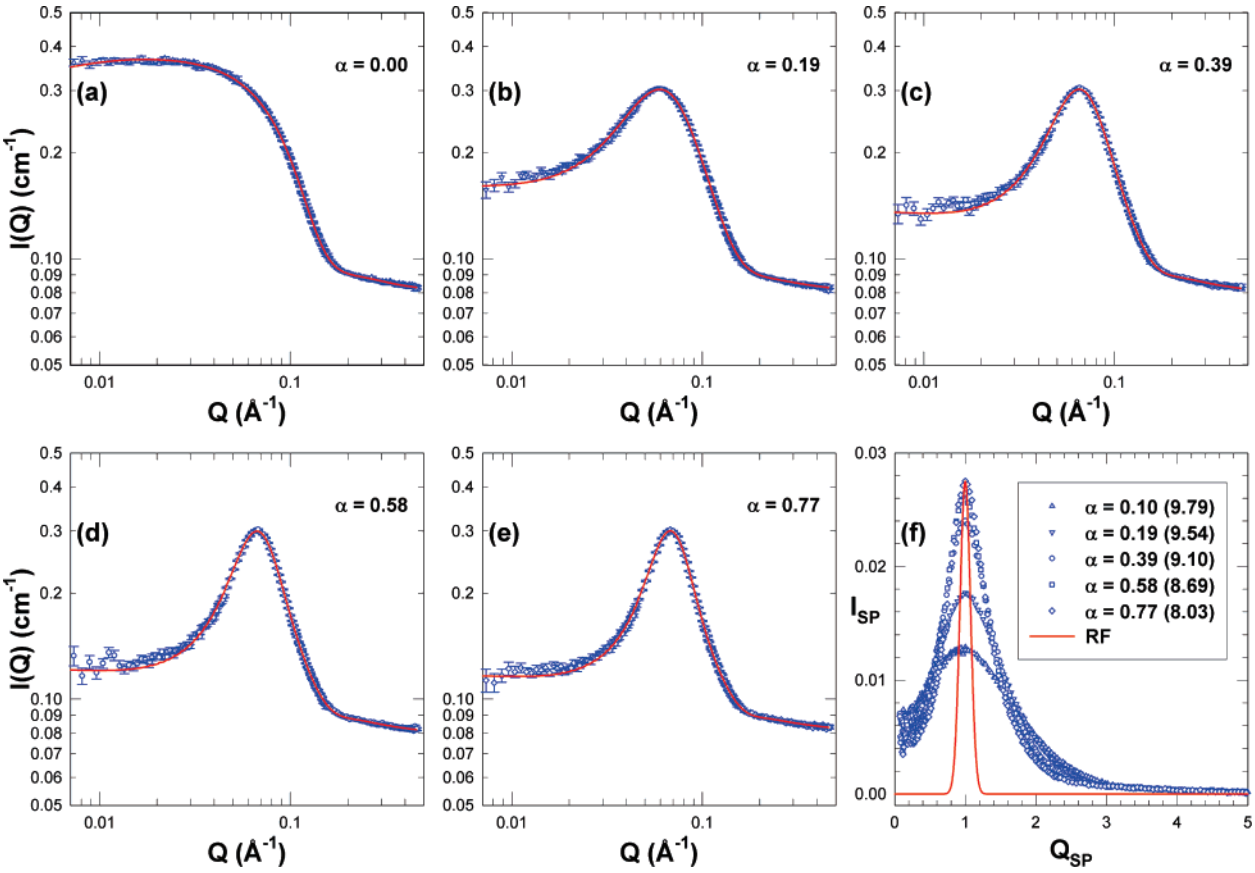

Figure 4. Theoretical fits to the SANS experimental data obtained from PAMAM dendrimers of generation 4 in D_2O solutions with concentration of 0.0225 g/mL in a α range from 0 to 0.77 (the corresponding pD values range from 9.79 to 8.03 and are displayed in parentheses in panel f). The experimental SANS intensity distributions are taken on the NG-3 SANS spectrometers at NIST CNR. Within this α range, a gradual building up of the local ordering, due to the incremental enhancement of the Coulombic repulsion, is clearly seen. In panel f, RF stands for the resolution function. The definitions of I_{SP} and Q_{SP} are given in the text.

are being charged ($0.97 < \sigma < 1.73$), the intramolecular structure keeps on evolving from a more diffusive picture toward more dense-packed conformation. The parameter a_b, appearing in the model of the dendrimer form factor $P(Q)$ given by eq 2, is defined as the normalized weighting factor of the scattering contribution of the intramolecular scattering density fluctuation to the contribution from the sphere with the density profile characterized by Gaussian density distribution and diffuse edge. Its dependence on α is presented in the inset. A smooth decrease is also seen to take place around $\alpha < 1$. These results are expected and consistent with our previous analysis as the tertiary amine groups are being protonated when $\alpha \sim 1$.

A further evidence of the possible internal structural changes can be seen by the looking at the evolution of the SANS intensity distribution $I(Q)$ at higher Q values with added DCl. Figure 7 shows its variation for the Q value ranging from 0.1 to 0.5 $Å^{-1}$. Experimentally it is found that the addition of DCl gradually induces the formation of the bump centered around $Q = 0.2$ $Å^{-1}$, which becomes more and more discernible upon increasing α. The intra-structure factor $P(Q)$ obtained by model fitting given in the insets clearly shows that when the tertiary amino groups begin to be protonated, the small bump becomes more and more pronounced, which implies a transition of the molecular conformation.

Intermolecular Interaction. Before detailing the model fitting results regarding the effective inter-dendrimer interaction, it is instructive to comment on the strengthening of the correlation peak of the SANS intensity distributions given in Figure 4, which is attributed to the gradual increase of the molecular protonation level by adding DCl within α ranging from 0 to 0.77 (the corresponding range of pD values varies from 10.25 to 8.03): It is well-known that the absolute scattering intensity obtained from a two-phase system, such as dendrimer molecules and D_2O in this specific case, is given by the Fourier transform of the Debye correlation function $\Gamma(r/\Lambda)$ with a length scale, Λ, characteristic of the system.[58] It is further demonstrated that the degree of local order can be visualized by transforming the SANS intensity distribution $I(Q)$ to this dimensionless rescaled scattering intensity distribution I_{SP}.[50−52] To be more specific, the I_{SP} given in panel 4f and 5f is defined as

$$I_{SP}(Q_{sp}) \equiv \int_0^\infty dR_{SP}\, 4\pi {R_{SP}}^2 \frac{\sin(R_{SP}Q_{SP})}{R_{SP}Q_{SP}} \Gamma(R_{SP}) = \frac{{Q_{MAX}}^3 I(Q\Lambda)}{\langle \eta^2 \rangle} \quad (26)$$

where $\langle \eta^2 \rangle$ is the so-called scattering invariant and defined as

$$\langle \eta^2 \rangle = \frac{1}{2\pi^2} \int_0^\infty Q^2 I(Q)\, dQ \quad (27)$$

where $\Gamma(x)$ is the Debye correlation function, $R_{SP} \equiv (r)/(\Lambda)$, $Q_{SP} \equiv Q\Lambda$, and $Q_{MAX} \equiv 1/\Lambda$, the peak position of the SANS intensity distribution.

Within this α range, the gradual increment of I_{SP} suggests that the enhancement of the electrostatic repulsion induces the formation of significant local ordering around any given protonated dendrimer molecule in the solution. The same feature is shared by the globular protein solutions at certain pH values

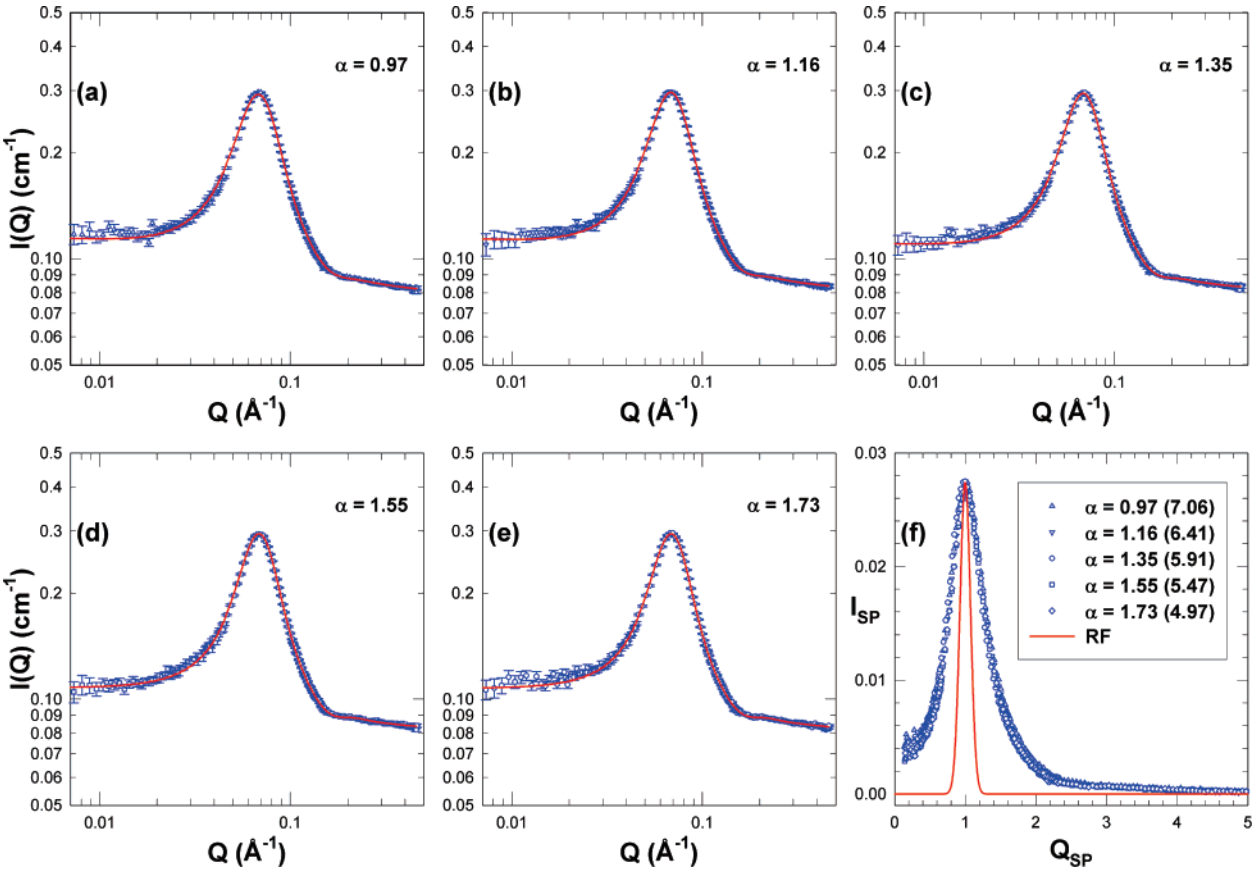

Figure 5. Same as Figure 3 but in a different α range. Unlike the previous Figure, within this α range ($0.97 < \alpha < 1.73$,$7.06 > pD > 4.97$), all the SANS intensity distributions are essentially identical to each other. It can be clearly seen from panel f that the local order and the inter-dendrimer interaction in solutions remain unchanged even with the progressive increment of the deuteron concentration in the solution and the degree of dendrimer molecular protonation. It can also be noticed that all the scaled curves are significantly broader than the resolution function of the NG3 spectrometer, indicating that the great similarity of the SANS intensity distributions is not resolution limited.

and other like-charged colloidal suspensions such as ionic micellar solutions.[30,59]

However, a completely different scenario is observed when $\alpha > 0.97$: Although the physicochemical condition of the PAMAM dendrimer solutions is expected to keep changing due to the progressive introduction of DCl, it is experimentally found that, as shown in Figure 5, within the α range of 0.97 to 1.73, the SANS intensity distributions are essentially identical to each other. The associated scaling plot, given in Figure 5f, indicates that all the rescaled intensity distributions collapse into one single master curve, indicating that the degree of the local order is invariant to the change of pD value of the solutions and suggesting that the inter-dendrimer interaction, which is sensitively susceptible to the variation of the effective charge carried by the dendrimer molecule and the ionic strength of the medium, remains unchanged. It is useful to point out that the rescaled curves being much broader than the instrument resolution (red solid line in Figures 4f and 5f) reflects a physical reality, and it is not due to the constraint of the resolution.

The average number of the protonated amino groups (structure charge) for a single dendrimer molecule as a function of α can be calculated by the constraint of charge neutrality incorporating the correction of deuteron activity, and the results are given in Figure 8 and its associated inset. It is experimentally found that the peripheral primary and internal tertiary amino groups of the G4 PAMAM dendrimers have different intrinsic proton binding constant (pK).[60−61] For pD values ranging from 10 to 7, most of the protonation is attributed to the primary amino groups, while the onset of the protonation of tertiary groups is reported at a pD of about 6.4 ($\alpha \approx 1.0$), indicated by a discernible change in the slope of the two protonated amino groups curves given in the inset of Figure 8.[62] Consequently a nearly linear increase of the overall protonation level as α evolves from 0 to 1.73 is obtained by a calculation based on the overall charge neutrality.

What is not available from this mathematical relationship is the average effective charge carried by a dendrimer molecule, an essential parameter determining the effective interaction between dendrimers in solutions, along with the ionic strength of the medium and the dendrimer volume fraction. By fitting the SANS experimental results with our model detailed in section II, the effective charge number of a dendrimer is expressed as a function of α in Figure 8. The difference between the effective charge and structural charge is the number of counterions associated with each dendrimer. In our case, the only type of counterions is chloride. Unlike the number of protonated amino groups, the extracted effective charge exhibits a completely different pD-dependent deuteron binding effect: Upon increasing the molecular protonation the effective charge is characterized by a steady increment when α ranges from 0 to 0.97.

When $\alpha > 0.97$, the effective charge as a function of α is seen to reach a plateau region with a constant value of about 32, while the number of counterions associating with a dendrimer molecule is about 110 at $\alpha = 1.73$. The strong association of counterions is expected to significantly influence the electrostatic repulsion among the charged amino groups. Therefore, the proper treatment of counterion association in a dendrimer in a computer simulation is critical to accurately predict the structural changes of a dendrimer molecule.

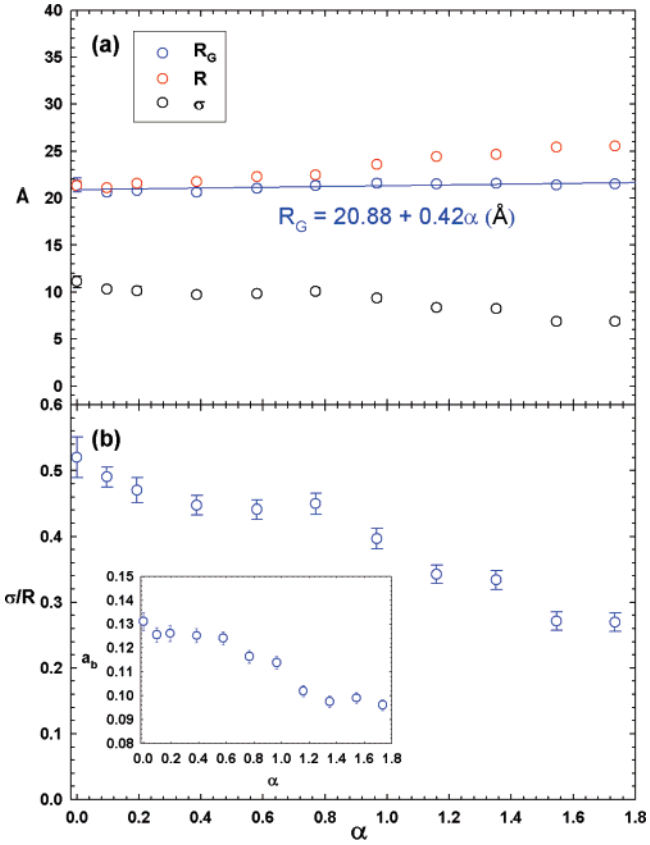

Figure 6. (a) Molecular conformation of PAMAM dendrimers of generation 4 in D_2O solutions with concentration of 0.0225 g/mL under various pD conditions obtained by SANS experiment and data analysis. The variation of the intra-particle structure factor $P(Q)$ parameters R, σ, radius of gyration R_G and its corresponding calibration curve as a function of α are presented. Note that the error bars are smaller than the symbol size. (b) Ratio of σ to R as a function of α. The relationship between weighting parameter a_b of intra-dendrimer form factor $P(Q)$ and α is given in the inset of the bottom panel. A transition is observed when $\alpha = 0.97$.

Another important parameter influencing the dendrimer interaction, the ionic strength of the medium defined by eq 22, is given in Figure 9 as a function of α. Its comparison to the curve representing the ionic strength of the medium without counterion association once again reflects the importance of incorporating the effect of counterion association in describing the effective interaction between the charged dendrimer molecules in solutions. Similar to the effective charge, the ionic strength of the medium is seen to gradually reach a constant value of about 0.025 when $\alpha > 0.97$.

Figure 10 displays the ratio of the number of chloride ions associated with the dendrimer molecules to the total number of chloride ions added into the solutions. Our discovery is in quantitative agreement with the results obtained from the theoretical men-field calculations, which reports this ratio within the pH range corresponding to $0 < \alpha < 1.0$,[57] but essentially different from the computer simulation results by Maiti and coworkers,[12] which report as 15% for "neutral pH" and 30% for "low pH" respectively, corresponding roughly to $\alpha = 1.0$ and $\alpha = 2.0$ in our experiments. The apparent discrepancy between the experimental and computational results is attributed to the different definition employed for the "internal chlorides". In the current model, the effective charge and equivalently the number of associated counterion are calculated through the effective inter-dendrimer interaction potential, which is assumed to be a Yukawa-like potential and can be directly calculated. Therefore, the effective charge is the net charge of a dendrimer molecule within a boundary, beyond which the interaction potential is described by the Yukawa form. This boundary should also include both the interior of a dendrimer and the so-called Stern layer. In our current model, the definition of hard-core radius is considered as a cutoff boundary, which is set as $R/2 = R_G$. The choice is based on the suggestion of the MD simulation and the best fitting to the experimental curves.[41]

It is important to understand why the effective charge remains invariant when $0.97 < \alpha < 1.73$. In general, the difference between the structural charge and effective charge for charged colloidal suspensions has been traditionally attributed to the counterion condensation.[43] It has been indicated that for a charged hard sphere particle, within the framework of PB theory, the effective charge will eventually saturate under conditions of high structural charge,[63] which seems to agree with our observation. However, unlike hard-sphere systems, the openness of the intramolecular structure and presence of the internal cavity allow the penetration and residence of the counterions. To understand the problem of the counterion distribution for the dendrimer solutions, it is therefore essential to consider the effect due to this unique structural property.

As shown in Figure 5, all scattering intensity distributions obtained from $0.97 < \alpha < 1.73$ are essentially identical with each other. This similarity suggests that the effective inter-dendrimer interaction, a collective manifestation of the effective charge and the ionic strength of the medium, remains intrinsically unchanged within this α range where the increase of the structural charge is mainly contributed by the protonation of the tertiary amino groups.[60] It is speculated that this observation is closely related to the difference in the physical mechanism of binding with counterions between the protonated tertiary amino groups and primary ones, as well as the general result due to the counterion condensation theory, which predicts that the effective charge carried by a hard-sphere colloid may reach a saturation value when the structural charge is high enough.[63]

The physical location of different amino groups is conjectured to be another possibility contributing to this observation: In comparison to the primary amino groups, the majority of the tertiary ones may reside well inside the molecular internal region. The association/dissociation rate of the chloride with the protonated tertiary amino groups may be affected significantly by the dynamics of the water molecules confined in the dendrimer molecule, which has been shown computationally to have much slower dynamical relaxation behavior compared with the bulk water.[18] Within the α range where the tertiary amino groups are protonated, as long as the chloride ions remain inside the dendrimer due to the dynamical and geometrical constraint, the effective inter-dendrimer interaction is not sensitive to their association or dissociation with the amino groups and therefore it is not possible for SANS experiments and current model fitting to differentiate them. Furthermore, other factors, such as the steric hindrance effect,[64] namely the difference of the available local space around these two amino groups to accommodate the chloride anions and the associated bound water molecules, are conjectured to contribute collectively to this selection rule of binding as well.

V. Conclusions

In this paper, we have applied our model to study the SANS intensity distribution $I(Q)$ for the charged G4 PAMAM dendrimers, with tunable molecular protonation due to the presence of the peripheral primary and interior tertiary amino groups, in D_2O solutions with low dendrimer concentration. On the basis of a model for the SANS absolute intensity which incorporates

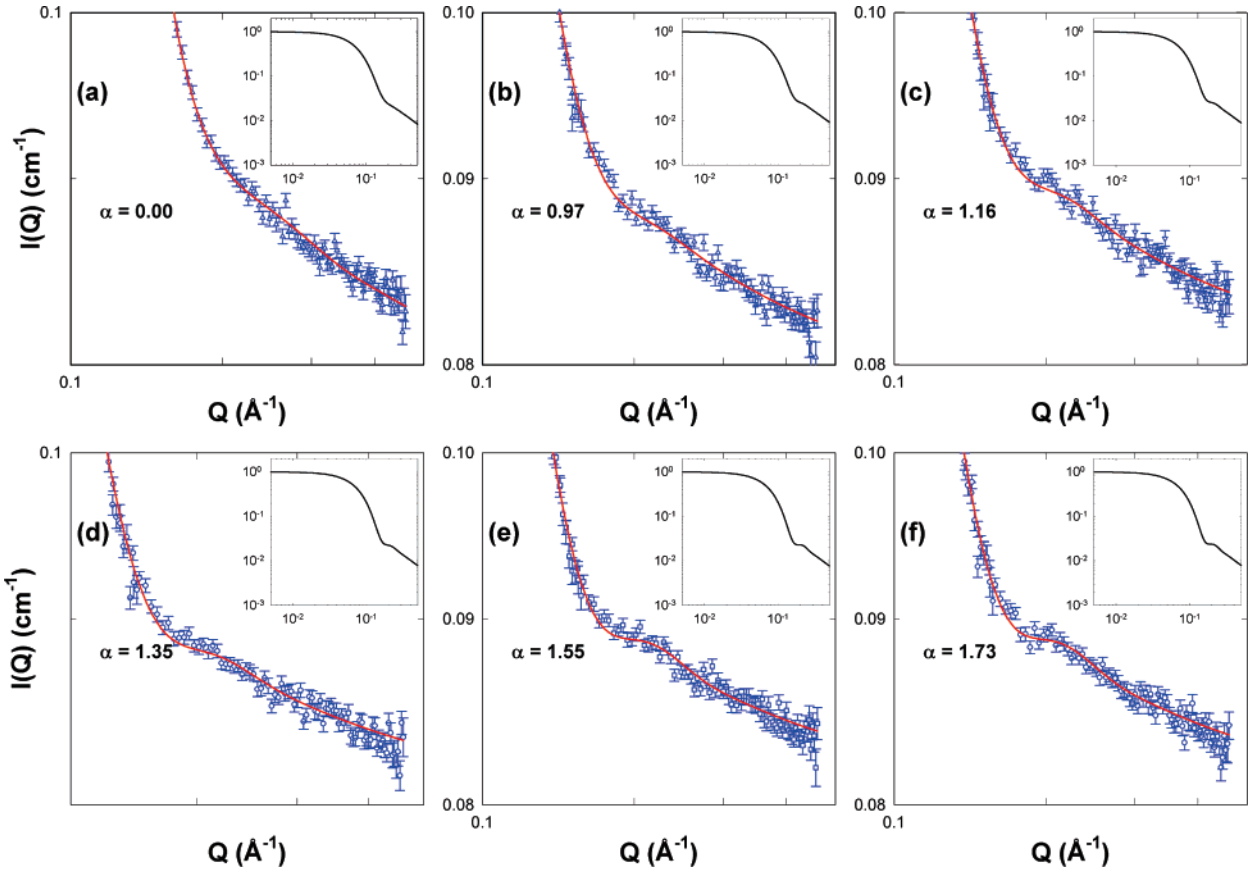

Figure 7. Comparison of the SANS intensity distributions $I(Q)$ when $Q > 0.1$ Å^{-1}, obtained from PAMAM dendrimers of generation 4 in D_2O solutions with concentration of 0.0225 g/mL with different α values, with the theoretical model described in section III. Note the evolution of $P(Q)$ presented in the insets: Upon increasing α, a gradual formation of a discernible bump around $Q = 0.2$ Å^{-1} is observed.

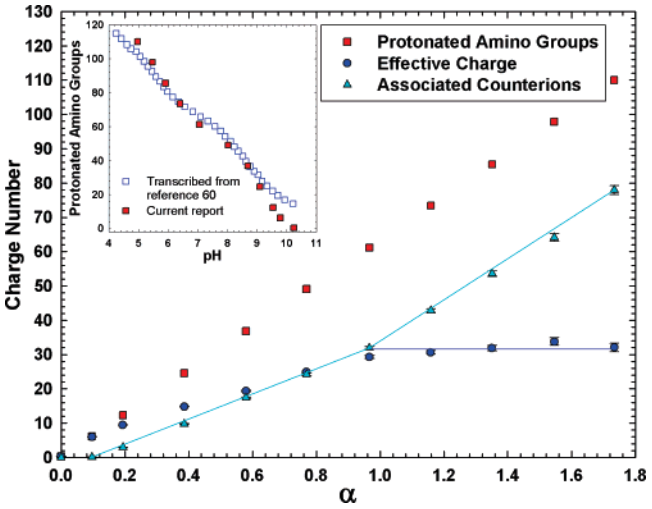

Figure 8. Average numbers of protonated amino groups, effective dendrimer molecular charges and the number of counterions associated with a dendrimer molecule as a function of α. A nearly linear increase of the molecular protonation is calculated from the overall charge neutrality; the effective charge carried by a dendrimer molecule is obtained from the SANS model fittings with OZ-HNC-GOCM approach. Upon increasing α, the effective charge is characterized by a steady increment when $\alpha < 1.0$ followed by an α independent region when $\alpha > 0.97$. The associated counterions curve exhibits a clear pD-dependent behavior as a discernible change in the slope when $\alpha = 0.97$ is observed. Solid lines are used to guide reader's eyes. The inset gives the relationship between the numbers of protonated amino groups and the pH value of the solutions, reported by Niu et al. in ref 60 and our current results. See text for details.

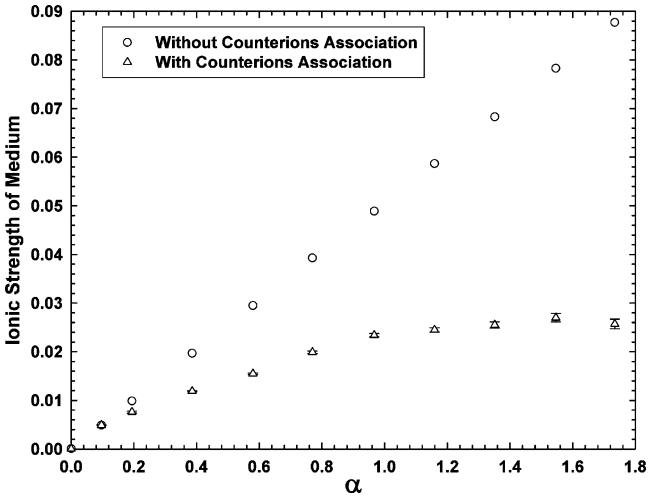

Figure 9. Tonic strength of the medium as a function of α. The red symbols represent the ionic strength without incorporating the counterion association. The blue symbols give the same quantity but with the correction of counterion association. Upon increasing α, the two curves progressively differ from each other. When $\alpha > 0.97$ more than 50% difference is observed, clearly illustrating the importance of fitting the SANS data with the counterion association effect taken into account properly.

(1) the inter-particle structure factor $S(Q)$ obtained by numerically solving the Ornstein−Zernike integral equation (OZ) with the hypernetted chain closure (HNC) for the screened Coulombic interaction potential, (2) the intra-particle structure factor $P(Q)$ for the modified fuzzy ball model with diffuse edges, (3) the effect of counterion association to obtain the correct ionic strength of the medium, (4) the generalized one-component macroion theory to relate the fitted potential parameters with the effective charge, and (5) the conversion of the measured

Table 1. Number of Protonated Amino Groups, Number of Effective Charge, and Number of Associated Counterions Per G4 PAMAM Dendrimer Molecule and the Fraction of Added Chlorides Associating to Dendrimers to Total Counterions, and Radius of Gyration at Various Solution Conditions Obtained by SANS Model Fittings[a]

pD	α	no. of protonated amino groups	no. of effective charges	no. of associated counterions	fraction of added chlorides associating with dendrimers	radius of gyration (Å)
10.25	0.00	0.29	0.29 ± 0.02	0.00 ± 0.02	0	21.41 ± 0.74
9.79	0.10	6.14	6.01 ± 0.04	0.13 ± 0.04	0.02 ± 0.01	20.64 ± 0.38
9.54	0.19	12.32	9.44 ± 0.08	2.88 ± 0.08	0.23 ± 0.01	20.83 ± 0.31
9.10	0.39	24.57	14.81 ± 0.12	9.75 ± 0.12	0.40 ± 0.01	20.63 ± 0.36
8.69	0.58	36.81	19.37 ± 0.19	17.44 ± 0.19	0.47 ± 0.01	21.02 ± 0.37
8.03	0.77	49.06	24.87 ± 0.31	24.19 ± 0.31	0.49 ± 0.01	21.34 ± 0.40
7.06	0.97	61.19	29.24 ± 0.42	31.95 ± 0.42	0.52 ± 0.01	21.58 ± 0.41
6.41	1.16	73.44	30.68 ± 0.55	42.76 ± 0.55	0.58 ± 0.01	21.49 ± 0.29
5.91	1.35	85.44	31.88 ± 0.78	53.57 ± 0.78	0.63 ± 0.01	21.56 ± 0.30
5.47	1.55	97.87	33.75 ± 1.10	64.12 ± 1.10	0.66 ± 0.01	21.40 ± 0.24
4.97	1.73	110.00	32.06 ± 1.26	77.94 ± 1.26	0.64 ± 0.01	21.49 ± 0.25

[a] Shown is also α, the ratio of moles of acid to the moles of the amino groups at different pD values of the solutions.

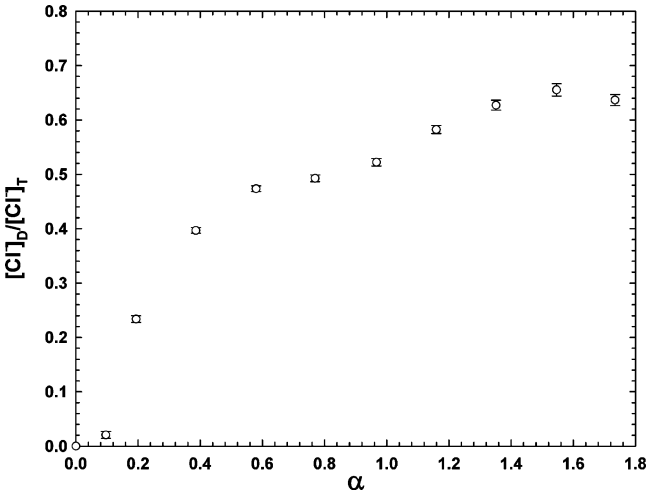

Figure 10. Fraction of chloride ions associating with the dendrimers ($[Cl^-]_D$) to the total chloride ions added in the solutions ($[Cl^-]_T$) as a function of α. A steady increase within the range of α from 0 to 0.98 reflects the increment of Coulomb attraction between the gradually protonated primary amino groups and the chloride anions. An increase of $[Cl^-]_D/[Cl^-]_T$ when $\alpha > 0.97$ is attributed to the preferred pairing between the chloride anions with the ionized tertiary amino groups.

deuteron activity to its real concentration, we demonstrate an good agreement between the extensive SANS intensity distributions obtained from a series of charged dendrimers solutions at 0.0225 g/mL with different degrees of molecular protonation, and the model of $I(Q)$ with reasonable and meaningful physical parameters.

Our research elucidates the effect of pD on the molecular conformation of PAMAM dendrimers in aqueous solutions. Systematic SANS data analysis qualitatively verifies the molecular swelling upon addition of acid, which is predicted by various computational studies. However, a quantitative dissimilarity is apparent: it is found that the dependence of the molecular conformation on the pD of solution is only about 4%, significantly less than MC and MD predictions,[65] but consistent with a recent theoretical calculation.[57] Although R_G of the dendrimer molecule is insensitive to the variation of the pD value of the solutions, we found that there is an internal structural change of a dendrimer during the protonation of the tertiary amino groups and the subsequent counterion association and penetration of water molecules collectively.

In particular, our systematic SANS data analysis reveals a pD-dependent behavior: upon adding DCl into the solutions, the number of counterions associated with a dendrimer is first progressively increased due to the protonation of dendrimers. When $0.97 < \alpha < 1.73$, despite the increasing molecular protonation, an invariance of the effective charge is observed. At present, it is attributed to the several possible origins, such as nonlinear accumulation of counterions, the dynamical constraint of the chloride ions inside the dendrimer molecule, and the influence of the steric hindrance effect.

In summary, based on the current SANS experimental evidence, these aforementioned hypotheses seem to provide reasonable explanations from different aspect for understanding the inter-dendrimer interaction at their charged state. More experimental measurements are currently under investigation to have better understanding of the coherent physical picture.

Acknowledgment. This research is partially based upon work by L.J.M. while serving at the National Science Foundation. W.R.C. thanks the National Science Foundation (CHE0316132) for financial support; Y.L. acknowledges partial financial support by the DOE within the Center of Excellence on Carbon-based Hydrogen Storage Materials. We also acknowledge the support of the National Institute of Standards and Technology, U.S. Department of Commerce, in providing the neutron research facilities supported under NSF Agreement DMR-0454672.

References and Notes

(1) Tomalia, D. A. *Chem. Today* **2005**, *23*, 41−45.
(2) Esfand, R.; Tomalia, D. A. *Drug. Discov. Today* **2001**, *6*, 427−436.
(3) Meijer, E. W.; van Genderen, M. H. P. *Nature (London)* **2003**, *426*, 128−129.
(4) Helms, B.; Meijer, E. W. *Science* **2006**, *313*, 929−930.
(5) Lee, C. C.; MacKay, J. A.; Fréchet, J. M. J.; Szoka, F. C. *Nat. Biotechnol.* **2005**, *23*, 1517−1526.
(6) Tomalia, D. A.; Baker, H.; Dewald, J.; Hall, M.; Kallos, G.; Martin, S.; Roeck, J.; Ryder, J.; Smith, P. *Polym. J.* **1985**, *17*, 117−132.
(7) Boas, U.; Heegaard, P. M. H. *Chem. Soc. Rev.* **2004**, *33*, 43−63.
(8) Bosman, A. W.; Janssen, H. M.; Meijer, E. W. *Chem. Rev.* **1999**, *99*, 1665−1688.
(9) Welch, P.; Muthukumar, M. *Macromolecules* **1998**, *31*, 5892−5897.
(10) Lee, I.; Athey, B. D.; Wetzel, A. W.; Meixner, W.; Baker, J. R. *Macromolecules* **2002**, *35*, 4510−4520.
(11) Terao, T.; Nakayama, T. *Macromolecules* **2004**, *37*, 4686−4694.
(12) Maiti, P. K.; Çağin, T.; Lin, S.-T.; Goddard, W. A. *Macromolecules* **2005**, *38*, 979−991.
(13) Lee, I.; Baker, J. R.; Larson, R. G. *J. Phys. Chem. B* **2006**, *110*, 4014−4019.
(14) Gurtovenko, A. A.; Lyulin, S. V.; Karttunen, M.; Vattulainen. I. *J. Chem. Phys.* **2006**, *124*, 094904-1−094904-8.
(15) Opitz, A. W.; Wagner, N. J. *J. Polym. Sci., B: Poly. Phys.* **2006**, *44*, 3062−3077.
(16) Terao, T. *Mol. Phys.* **2006**, *104*, 2507−2513.
(17) Maiti, P. K.; Goddard, W. A. *J. Phys. Chem. B* **2006**, *110*, 25628−25632.
(18) Lin, S.-T.; Maiti, P. K.; Goddard, W. A. *J. Phys. Chem. B* **2005**, *109*, 8663−8672.

(19) For example, see the comments available in refs 14, 32, and 33 of the current paper.
(20) Nisato, G.; Ivkov, R.; Amis, E. J. *Macromolecules* **2000**, *33*, 4172−4176.
(21) Hansen, J.-P.; McDonald, I. R. *Theory of Simple Liquids*, 3rd ed.; Academic Press: Amsterdam, 2006.
(22) Ramzi, A.; Scherrenberg, R.; Brackman, J.; Joosten, J.; Mortensen, K. *Macromolecules* **1998**, *31*, 1621−1626.
(23) Nisato, G.; Ivkov, R.; Amis, E. J. *Macromolecules* **1999**, *32*, 5895−5900.
(24) Ohshima, A.; Konishi, T.; Yamanaka, J.; Ise, N. *Phys. Rev. E* **2001**, *64*, 051808-1−051808-9.
(25) Ramzi, A.; Scherrenberg, R.; Joosten, J.; Lemstra, P.; Mortensen, K. *Macromolecules* **2002**, *35*, 827−833.
(26) In their own activities as scientific institutions, NIST and ORNL use many different materials, products, types of equipment, and services. However, NIST and ORNL do not approve, recommend, or endorse any product or proprietary material.
(27) In the text of the current report, the word "protonation" is used to describe the binding between the deuterons and the amino groups.
(28) NIST Scientific and Technical Databases; National Institute of Standards and Technology Technical Services: Gaithersburg, MD.
(29) Kline, S. R. *J. Appl. Crystallogr.* **2006**, *39*, 895−900.
(30) Chen, S.-H. *Annu. Rev. Phys. Chem.* **1986**, *37*, 351−399.
(31) de Gennes, P. G.; Hervet, H. *J. Phys., Lett.* **1983**, *44*, L351−L360.
(32) Ballauff, M.; Likos, C. N. *Angew. Chem. Int.* **2004**, *43*, 2998−3020.
(33) Likos, C. N.; Ballauff, M. *Top. Curr. Chem.* **2005**, *245*, 239−252.
(34) Likos, C. N. *Soft Matter* **2006**, *2*, 478−498.
(35) Lescanec, R. L.; Muthukumar, M. *Macromolecules* **1990**, *23*, 2280−2288.
(36) Rathgeber, S.; Monkenbusch, M.; Kreitschmann, M.; Urban, V.; Brulet. A. *J. Chem. Phys.* **2002**, *117*, 4047−4062.
(37) Pedersen, J. S. *J. Chem. Phys.* **2001**, *114*, 2839−2846.
(38) Hashimoto, T.; Todo, A.; Itoi, H.; Kawai, H. *Macromolecules* **1977**, *10*, 377−384.
(39) Strey, R.; Winkler, J.; Magid, L. *J. Phys. Chem.* **1991**, *95*, 7502−7507.
(40) Gradzielski, M.; Langevin, D.; Magid, L.; Strey, R. *J. Phys. Chem.* **1995**, *99*, 13232−13238.
(41) As pointed out by ref 49 of the current report, in the dilute limit of the volume fraction of dendrimer molecules, for the $\alpha = 0$ case, the effective inter-dendrimer interaction can be justified as hard sphere-like potential with radius of $2R_G$. It is therefore reasonable to choose $2R_G$ as the effective diameter for any $\alpha > 0$ case. Namely, when $r < 2R_G$,$V_{eff}(r) = \infty$. When $r > 2R_G$, $V_{eff}(r)$ is described by the screened Coulombic potential with a Yukawa form. Attempts have also been made to test the validity of this implement by treating the effective radius as fitting parameter during the fitting procedures: It is found that the ratio of the fitted effective radius to R_G is generally between 1 and 1.06, with the equally good agreement, judging by the χ^2, between the SANS experimental results obtained at various α values and the model proposed in the current paper.
(42) Belloni, L. *J. Phys.: Condens. Matter* **2000**, *12*, R549−R587.
(43) Schmitz, K. S. *Macroions in Solution and Colloidal Suspension;* VCH Publishers: New York, 1993.
(44) For example, see: Boström, M.; Tavares, F. W.; Bratko, D.; Ninham, B. W. *J. Phys. Chem.* **2005**, *109*, 24489−24494 and references therein.
(45) Belloni, L. *J. Chem. Phys.* **1986**, *85*, 519−526.
(46) Chen, S.-H.; Sheu, E. Y. In *Micellar Solutions and Microemulsions−Structure, Dynamics, and Statistical Thermodynamics*; Chen, S.-H., Rajagopalan, R., Eds.: Springer-Verlag: New York, 1990.
(47) Verwey, E. J. W.; Overbeek, J. T. G. *Theory of Stability of Lyophobic Colloids;* Elsevier: Amsterdam, 1948.
(48) Pitzer, K. S. In *Activity Coefficients in Electrolyte Solutions*, 2nd ed.; Pitzer, K. S., Ed.; CRC Press: Boca Raton, FL, 1991.
(49) Likos, C. N.; Rosenfeldt, S.; Dingenouts, N.; Ballauff, M.; Lindner, P.; Werner, N.; Vögtle, F. *J. Chem. Phys.* **2002**, *117*, 1869−1877.
(50) Chen, W.-R.; Chen, S.-H.; Mallamace, F. *Phys. Rev. E* **2002**, *66*, 021403-1−021403-12.
(51) Chen, S.-H.; Chen, W.-R.; Mallamace, F. *Science* **2003**, *300*, 619−622.
(52) Chen, W.-R.; Mallamace, F.; Glinka, C. J.; Fratini, E.; Chen, S.-H. *Phys. Rev. E* **2003**, *68*, 041402-1−041402-15.
(53) Klein, R. In *Neutrons, X-rays and Light: Scattering Methods Applied to Soft Condensed Matter*; Lindner, P., Zemb, Th., Eds.; North-Holland: Amsterdam, 2002.
(54) Qamhieh, K.; Linse, P. *J. Chem. Phys.* **2005**, *123*, 104901-1−104901-12.
(55) Russ, C.; von Grünberg, H. H.; Dijkstra, M.; van Roij, R. *Phys. Rev. E* **2002**, *66*, 011402-1−011402-12.
(56) In the current paper, we only report the experimental results of 0.0225 g/mL of G4 PAMAM dendrimer solutions, in which the protonation of dendrimer molecules is established by progressively adding DCl into the solutions. Ongoing study indicates the current model also gives excellent agreements with the SANS data obtained from the low concentration PAMAM dendrimers of G4, G5, and G6 in D_2O with different acids, including DBr, DI, DNO_3, D_2SO_4, and D_3PO_4 used to protonate the amino groups. The reports of these works are under preparation.
(57) Govorun, E. N.; Zeldovich, K. B.; Khokhlov, A. R. *Macromol. Theory Simul.* **2003**, *12*, 705−713.
(58) Debye, P.; Bueche, A. M. *J. Appl. Phys.* **1949**, *20*, 518−525.
(59) Tardieu, A.; Le Verge, A.; Malfois, M.; Bonnete, F.; Finet, S.; Ries-Kautt, M.; Belloni, L. *J. Cryst. Growth* **1999**, *196*, 193−203.
(60) Niu, Y.; Sun, L.; Crook, R. M. *Macromolecules* **2003**, *36*, 5725−5731.
(61) van Duijvenbode, R. C.; Borkovec, M.; Koper, G. J. M. *Polymer* **1998**, *39*, 2657−2664.
(62) The slightly quantitative disagreement between the protonation level reported in the current paper and ref 60 shown in the inset is attributed to the difference of the absolute pH value for a given sample obtained by different pH meters and the isotope effect.
(63) Belloni, L. *Colloids Surf. A* **1998**, *140*, 227−243.
(64) Pauling, L. C. *Chemistry;* W. H. Freeman & Co.: New York, 1975.
(65) It is important to note that in the computational studies the radius of gyration R_G is calculated in terms of the atomic mass of the constituting components of the PAMAM dendrimer molecule. In SANS experiments R_G is weighted by the neutron scattering cross sections.

MA0626564